Prolonged niacin treatment leads to increased adipose tissue PUFA synthesis and anti-inflammatory lipid and oxylipin plasma profile[S]

Mattijs M. Heemskerk,[1,*,†] Harish K. Dharuri,[1,2,*,†] Sjoerd A. A. van den Berg,[3,*,†] Hulda S. Jónasdóttir,[§] Dick-Paul Kloos,[§] Martin Giera,[§] Ko Willems van Dijk,[*,†,] and Vanessa van Harmelen[4,*,†]**

Department of Human Genetics,* Einthoven Laboratory for Experimental Vascular Medicine,[†] Center for Proteomics and Metabolomics,[§] and Department of Internal Medicine,** Leiden University Medical Center, Leiden, The Netherlands

Abstract **Prolonged niacin treatment elicits beneficial effects on the plasma lipid and lipoprotein profile that is associated with a protective CVD risk profile. Acute niacin treatment inhibits nonesterified fatty acid release from adipocytes and stimulates prostaglandin release from skin Langerhans cells, but the acute effects diminish upon prolonged treatment, while the beneficial effects remain. To gain insight in the prolonged effects of niacin on lipid metabolism in adipocytes, we used a mouse model with a human-like lipoprotein metabolism and drug response [female APOE*3-Leiden.CETP (apoE3 Leiden cholesteryl ester transfer protein) mice] treated with and without niacin for 15 weeks. The gene expression profile of gonadal white adipose tissue (gWAT) from niacin-treated mice showed an upregulation of the "biosynthesis of unsaturated fatty acids" pathway, which was corroborated by quantitative PCR and analysis of the FA ratios in gWAT. Also, adipocytes from niacin-treated mice secreted more of the PUFA DHA ex vivo. This resulted in an increased DHA/arachidonic acid (AA) ratio in the adipocyte FA secretion profile and in plasma of niacin-treated mice. Interestingly, the DHA metabolite 19,20-dihydroxy docosapentaenoic acid (19,20-diHDPA) was increased in plasma of niacin-treated mice. Both an increased DHA/AA ratio and increased 19,20-diHDPA are indicative for an anti-inflammatory profile and may indirectly contribute to the atheroprotective lipid and lipoprotein profile associated with prolonged niacin treatment.**—M. M. Heemskerk, H. K. Dharuri, S. A. A. van den Berg, H. S. Jónasdóttir, D-P. Kloos, M. Giera, K. Willems van Dijk, and V. van Harmelen. **Prolonged niacin treatment leads to increased adipose tissue PUFA synthesis and anti-inflammatory lipid and oxylipin plasma profile.** ***J. Lipid Res.*** **2014.** 55: **2532–2540.**

Supplementary key words drug therapy/hypolipidemic drugs • adipocytes • fatty acid/biosynthesis • omega-3 fatty acids • cytochrome P450 • polyunsaturated fatty acid

Niacin (vitamin B3) treatment reduces CVD and atherosclerosis development (1). These beneficial effects are mediated, in part, by lowering circulating levels of LDL-cholesterol, VLDL-TG, and lipoprotein(a) (2), as well as by increasing HDL-cholesterol (3). In addition, prolonged niacin treatment also decreases plasma, adipose tissue, and vascular inflammation (4, 5), which might contribute to reducing CVD. The induction of these beneficial effects after prolonged niacin treatment is in striking contrast to the unwanted acute niacin effects.

Acutely, niacin binds to the inhibitory hydroxycarboxylic acid receptor 2 (HCA_2) (previously known as GPR109A). In adipocytes, this leads to an inhibition of adipocyte lipolysis followed by an acute reduction of plasma nonesterified fatty acid (NEFA) levels. Lowering NEFA levels causes metabolic stress (6, 7), which increases stress hormone levels (8–12) after niacin treatment. In the skin Langerhans cells and keratinocytes, acute niacin binding to the

This work was supported by grants from Center of Medical Systems Biology (CMSB), the Netherlands Consortium for Systems Biology (NCSB) established by The Netherlands Genomics Initiative/Netherlands Organization for Scientific Research (NGI/NWO), Leiden University Medical Center (LUMC). H. S. Jónasdóttir is partially funded by the Stichting Prof. Jan Veltkamp Fonds (LUMC). This study was performed within the framework of the Center for Translational Molecular Medicine (http://www.ctmm.nl), project PREDICCt (Grant 01C-104). The authors declare that there is no conflict of interest associated with this manuscript.

Manuscript received 12 June 2014 and in revised form 13 October 2014.

Published, JLR Papers in Press, October 15, 2014
DOI 10.1194/jlr.M051938

Abbreviations: 14(15)-EpETE, 14(15)-epoxy eicosatetraenoic acid; 19(20)-EpDPA, 19(20)-epoxy docosapentaenoic acid; 19,20-diHDPA, 19,20-dihydroxy docosapentaenoic acid; AA, arachidonic acid; ALA, α-linolenic acid; APOE*3-Leiden.CETP, apoE3 Leiden cholesteryl ester transfer protein; COX, cyclooxygenase; CYP, cytochrome P450; FDR, false discovery rate; gWAT, gonadal white adipose tissue; NEFA, nonesterified fatty acid; qPCR, quantitative PCR.

[1] M. M. Heemskerk and H. K. Dharuri contributed equally to this article.
[2] Present address of H. K. Dharuri: Illumina Inc., Hayward, CA.
[3] Present address of S. A. A. van den Berg: Department of Clinical Chemistry and Hematology, Amphia Hospital, Breda, The Netherlands.
[4] To whom correspondence should be addressed.
e-mail: v.j.a.van_harmelen@lumc.nl

[S] The online version of this article (available at http://www.jlr.org) contains supplementary data in the form of nine figures and five tables.

HCA_2 receptor leads to a release of arachidonic acid (AA) and subsequent cyclooxygenase (COX)-mediated oxylipin synthesis (mostly prostaglandins) causing flushing (13) and a decrease in blood pressure (14). Intriguingly, these acute effects decrease upon prolonged niacin treatment. Adipocyte lipolysis normalizes (15, 16) and flushing diminishes (17).

The fact that certain acute niacin effects decrease over time whereas the beneficial lipid-lowering and anti-inflammatory effects remain, suggests differences between the induction of intracellular signaling pathways upon acute and prolonged niacin treatment. In the current study, we set out to characterize changes in signaling regulation upon prolonged niacin treatment. We specifically investigated effects of niacin on adipose tissue as adipose tissue has been shown to be the most affected organ at the gene expression level after 7 h of niacin treatment (18).

We treated mice with 0.3% niacin mixed through the diet and isolated gonadal white adipose tissue (gWAT) after 15 weeks of intervention. The mice used in this study were female APOE*3-Leiden.CETP (apoE3 Leiden cholesteryl ester transfer protein) mice (19), which, in contrast to wild-type mice, have a human-like lipoprotein profile and respond similarly to atheroprotective drugs like niacin (20). A microarray was used to compare gene expression profiles in the adipose tissue. We applied bioinformatic and statistical analyses to the gene expression data and showed that prolonged niacin treatment led to an increase in the pathways of unsaturated FA synthesis. To investigate whether PUFA levels and possible derivatives thereof (i.e., oxylipins) were functionally affected, we determined the FA composition in the adipose tissue by GC-MS and measured PUFA and oxylipin profiles in plasma by LC-MS/MS.

MATERIALS AND METHODS

Mouse experiments

Female APOE*3-Leiden.CETP mice were bred at the Leiden University Medical Center, Leiden, The Netherlands. At age 15 ± 1 weeks, mice were fed a Western-type diet (Diet T with 0.1 g% cholesterol, which consisted of 16 kcal% protein, 43 kcal% carbohydrate, and 41 kcal% fat; AB Diets, Woerden, The Netherlands) with or without niacin (0.3 g%; Sigma Aldrich, St. Louis, MO). Supplementary Table II shows the FA composition of the diet. Body weight was registered weekly. Animals were housed in a controlled environment (21°C, 40–50% humidity) with a daily 12 h photoperiod (0700–1900). Food and tap water were available ad libitum during the whole experiment. Food intake was determined weekly by weighing the food in the cages at t = 0 and at t = 1 days. The difference between these time points was equal to 24 h food intake of the mice. The mice in this study are the same as in our previously published study (16). All experiments were performed after a 15 week dietary intervention period. All animals (n = 14 per group) were anesthetized and euthanized in the fed state between 0800 and 0930 by cardiac puncture. Organs and plasma were collected and stored at −80°C. Fresh gWAT was harvested and kept in PBS with or without niacin. One niacin-treated animal did not have sufficient gWAT for the analyses. All animal experiments were performed in accordance with the regulations of Dutch law on animal welfare. The institutional scientific committee and ethics committee for animal procedures from the Leiden University Medical Center approved the protocols.

gWAT gene expression analysis

RNA was isolated from gWAT using the Nucleospin RNA/Protein kit (MACHEREY-NAGEL GmbH and Co. KG, Düren, Germany), after which RNA quality was assessed by NanoDrop (NanoDrop) and 2100 BioAnalyzer (Agilent). All samples had an RNA integrity number of >7.5. cRNA was synthesized using the TotalPrep RNA Amplification Kit (Ambion, Illumina). cRNA levels were normalized to 150 ng/µl and loaded onto MouseWG-6 v2.0 Expression BeadChips by Service XS (Leiden, The Netherlands). Each BeadChip contains eight arrays. Hybridization and washing were performed according to the Illumina manual. Image analysis and extraction of raw expression data were performed with Illumina GenomeStudio v2011.1 gene expression software with default settings.

The lumi (21) module in the R-based Bioconductor package was used to read in the combined (average) signal intensities per probe. A variance-stabilizing transformation (lumiT) available in the R package was used to stabilize the expression variance based on the bead level expression variance and mean relations. Expression data were normalized using the function lumiN available within the lumi package. We used limma (22), an R-based Bioconductor package, to calculate the level of differential gene expression. In addition to determining significant differentially expressed genes, gene set analysis based on the KEGG pathway and Gene Ontology was performed using the Bioconductor package "GlobalTest" (23).

Quantitative PCR

RNA was isolated from gWAT and liver using the Nucleospin RNA/Protein kit (MACHEREY-NAGEL GmbH and Co. KG). Subsequently, 1 µg of RNA was used for cDNA synthesis by iScript (BioRad, Hercules, CA), which was purified by the Nucleospin Gel and PCR clean-up kit (MACHEREY-NAGEL). Real-Time PCR was carried out on the IQ5 PCR machine (BioRad) using the Sensimix SYBR Green RT-PCR mix (Quantace, London, United Kingdom) and QuantiTect SYBR Green RT-PCR mix (Qiagen, Venlo, The Netherlands). Target mRNA levels were normalized to *Rplp0* and *Ppia* mRNA levels. Primer sequences and PCR conditions can be found in supplementary Table I.

gWAT, liver, and diet FA composition

FA composition analysis of gWAT, liver, and diet was carried out as described recently by Kloos et al. (24). Briefly, triplicate samples were weighed of ~10 mg diet or organ from niacin-treated and control mice. One milliliter of water, 3 ml methanol, and 1 ml 10 M NaOH were added, and the samples were flushed with argon and hydrolyzed for 1 h at 90°C. After acidification with 2 ml of 6 M HCl, 10 µl of an internal standard solution ([$^2H_{31}$]palmitic acid and ergosterole 10 µg/ml each) was added. The samples were extracted twice with 3 ml *n*-hexane, and the combined organic extracts were dried under a gentle stream of nitrogen. Dried samples were derivatized using 25 µl of *N-tert.*-butyldimethylsilyl-*N*-methyltrifluoroacetamide (Sigma Aldrich, Schnelldorf, Germany) for 10 min at 21°C, subsequently 25 µl of *N,O*-bis(trimethylsilyl)trifluoroacetamide containing 1% trimethylchlorosilane (Thermo Scientific, Waltham, MA) and 2.5 µl of pyridine were added, and the sample was heated for 15 min to 50°C. Next, 947.5 µl of *n*-hexane, containing 10 µg/ml octadecane (C_{18}) as system monitoring component, was added. Samples were analyzed in SIM mode on a Scion TQ GC-MS (Bruker,

Bremen, Germany) equipped with a 15 m × 0.25 mm × 0.25 mm BR5MS column (Bruker). The injection volume was 1 μl, the injector was operated in splitless mode at 280°C, and the oven program was as follows: 90°C kept constant for 0.5 min, then ramped to 180°C with 30°C/min, then to 250°C with 10°C/min, then to 266°C with 2°C/min, and finally to 300°C with 120°C/min, kept constant for 2 min. Helium (99.9990%, Air Products, The Netherlands) was used as carrier gas. For data analysis, a total area correction was applied, and triplicates were averaged.

Gonadal adipocyte PUFA release assay

Fresh gonadal adipose tissue was minced and digested in 0.5 g/l collagenase type I in HEPES buffer (pH 7.4) with 20 g/l of dialyzed BSA (BSA, fraction V; Sigma Aldrich) for 1 h at 37°C. The disaggregated WAT was filtered through a nylon mesh with a pore size of 236 μm. For the isolation of mature adipocytes, cells were obtained from the surface of the filtrate and washed several times. Adipocytes (~10,000 cells/ml) were incubated in triplicate in a 96-well plate at 37°C in 200 μl per well of DMEM/F12 medium with 2% w/w BSA with or without niacin (10^{-6} M) for 2 h. The adipocyte conditioned medium (100 μl) was frozen at –20°C until further analysis.

Plasma PUFA and oxylipin measurement

Protein precipitation was performed on adipocyte-conditioned medium (80 μl) or plasma (20 μl) by the addition of methanol (233.6 μl for medium and 53.6 μl for plasma) and 6.4 μl of internal standard solution (containing [$^2H_8$]15-HETE, [$^2H_4$]PGE_2, [$^2H_4$]LTB_4, and [$^2H_5$]DHA, each 50 ng/ml in methanol), which was left to equilibrate for 20 min at –20°C. The samples were spun down for 10 min, 16,200 *g* at 4°C. Supernatant (240 μl for medium and 30 μl for plasma) was pipetted into a deactivated glass insert (Agilent, CA). Plasma supernatant was diluted in 30 μl of water, while medium supernatant was dried by Speedvac at room temperature. The dried medium sample was dissolved in 60 μl 1:2 methanol-water. For both sample types, 20 μl was injected for LC-MS/MS analysis as described previously (25, 26).

LC-MS/MS analysis was carried out on a QTrap 6500 mass spectrometer (AB Sciex, Nieuwerkerk aan den Ijssel, The Netherlands), coupled to a Dionex Ultimate 3000 LC-system including autosampler and column oven (Dionex part of Thermo, Oberschleißheim, Germany). The column used was a Kinetex C18 50 × 2.1 mm, 1.7 μm, protected with a C_8 precolumn (Phenomenex, Utrecht, The Netherlands). Water (A) and methanol (B) both with 0.01% acetic acid were used. The gradient program started at 40% eluent B and was kept constant for 1 min, then linearly increased to 45% B at 1.1 min, then to 53.5% B at 4 min, to 55% B at 6.5 min, then to 90% B at 12 min, and finally to 100% B at 12.1 min, kept constant for 3 min. The flow rate was set to 250.0 μl/min. The MS was operated under the following conditions: the collision gas flow was set to medium, the drying temperature was 400°C, the needle voltage was −4,500 V, the curtain gas was 30 psi, ion source gas 1 was 40 psi, and the ion source gas 2 was 30 psi (air was used as drying gas and nitrogen as curtain gas). For quantitation, the multiple reaction monitoring transitions and collision energies given in supplementary Table V were used combined with calibration lines. All substances used as standards were from Cayman Chemicals (Ann Arbor, MI) if not stated otherwise, except RvE1, RvE2, 18S-RvE3, and 18R-RvE3 (gifts from Dr. Makoto Arita, Tokyo, Japan). Metabolite identification in plasma was verified by MS/MS spectral comparison with standards, of which leukotriene E_4, thromboxane B_2, and 19,20-dihydroxy docosapentaenoic acid (19,20-diHDPA) are included in the supplementary data (supplementary Figs. IV–VI).

Statistics

Mean values and SDs are reported in all figures. The gene expression data were statistically analyzed by using the multiple test correction method of Benjamin-Hochberg for control of false discovery rate (FDR) for both differentially expressed individual genes and for KEGG pathways. An adjusted P value <0.05 was considered significant. Calculations for the lipid measurements were performed in Prism version 6 (GraphPad Software, La Jolla, CA). Multiple *t*-tests were performed, and a 5% FDR value was applied. An *F*-test was applied to test whether linear regression lines were significantly nonzero. The levels of significance were set at $P < 0.05$.

RESULTS

gWAT gene expression analysis

Female APOE3.Leiden.CETP mice (n = 14 per group) were fed a Western-type diet (containing 0.1% cholesterol) with and without niacin for 15 weeks. As previously published (16), niacin treatment did not lead to differences in body weight nor gWAT weight in these mice. However, plasma lipids (i.e., total cholesterol, TGs, and phospholipids) were all decreased (16). Gene expression analysis generated 24 differentially expressed genes due to niacin treatment after multiple test correction (adjusted $P < 0.05$, see **Table 1**). The global test was applied to identify KEGG pathways affected by niacin treatment. **Table 2** depicts the top five pathways identified by global test; however, only "biosynthesis of unsaturated fatty acids" remained significant after correction for false discovery rate ($q < 0.05$). The differentially expressed genes from Table 1 were clustered and highlighted according to KEGG pathways. The top hits from the "biosynthesis of unsaturated fatty acids" (*Elovl6*, *Tecr*, and *Elovl5*) were all specifically involved in FA elongation, not FA desaturation, and were all upregulated. Quantitative PCR (qPCR) measurements of *Elovl6* and *Elovl5* in gWAT confirmed upregulation of mRNA levels of these enzymes after niacin treatment (**Fig. 1**). The rate-limiting desaturase enzyme of PUFA synthesis encoded by *Fads2* (fatty acid desaturase 2) showed a trend toward increased expression after niacin.

gWAT FA composition and adipocyte PUFA secretion

To investigate whether the increased mRNA levels of genes in the "biosynthesis of unsaturated fatty acids" translated to adipose tissue FA metabolism changes, we examined the FA composition of the gWAT by GC-MS. In the adipose tissue, the fractions of the substrates for PUFA synthesis, the essential FAs α-linolenic acid (ALA, n-3) and linoleic acid (LA, n-6), were decreased after niacin treatment while their downstream products were not fractionally different (supplementary Fig. I and Table II). As the only source of essential FAs was the diet, of which the consumption was equal (data not shown), an increased enzymatic processing of essential FAs toward downstream elongated and desaturated PUFAs would be plausible. To examine enzymatic processing, we investigated the substrate/product ratios for the enzymes in the PUFA synthesis

TABLE 1. Differentially expressed gene hits from microarray analysis of gWAT after niacin treatment

Gene Symbol	Gene ID	Gene Name	Adjusted *P*	Log (Fold Change)
Pdzk1ip1	67182	PDZK1 interacting protein 1	0.002	1.190
Orm2	18406	Orosomucoid 2	0.002	0.857
Orm1	18405	Orosomucoid 1	0.003	0.550
Elovl6[a]	170439	Elongation of long chain fatty acids 6	0.004	1.371
Lctl	235435	Lactase-like	0.004	1.107
Rdh11	17252	Retinol dehydrogenase 11	0.007	0.887
Nudt7	67528	Nudix (nucleoside diphosphate linked moiety X)-type motif 7	0.012	0.537
Acat2	110460	Acetyl-CoA acetyltransferase 2	0.013	0.695
Mup3	17842	Major urinary protein 3	0.013	1.047
1500017E21Rik	668215	RIKEN cDNA 1500017E21 gene	0.013	0.612
Clstn3	232370	Calsyntenin 3	0.013	0.607
Apoc1	11812	Apolipoprotein C-I	0.013	0.523
Comt	12846	Catechol-*O*-methyltransferase	0.014	0.536
Zfp385b	241494	Zinc finger protein 385B	0.014	−0.436
Tecr[a]	106529	*Trans*-2,3-enoyl-CoA reductase	0.029	0.498
G6pdx	14381	Glucose-6-phosphate dehydrogenase X-linked	0.029	0.454
Elovl5[a]	68801	Elongation of long chain fatty acids 5	0.033	0.405
Pkm2	18746	Pyruvate kinase, muscle	0.034	0.521
D430019H16Rik	268595	RIKEN cDNA D430019H16 gene	0.034	−0.505
Aacs	78894	Acetoacetyl-CoA synthetase	0.035	0.524
Lpcat3	14792	Lysophosphatidylcholine acyltransferase 3	0.035	0.504
Kcnj15	16516	Potassium inwardly rectifying channel, subfamily J, member 15	0.035	0.450
Cyp51	13121	Cytochrome P450, family 51	0.039	0.747
Aard	239435	Alanine and arginine rich domain containing protein	0.039	−0.547
Fasn	14104	Fatty acid synthase	0.126	0.487
Acly	104112	ATP citrate lyase	0.139	0.691

P value after multiple testing correction. The fold change was calculated as $\log_2$ (niacin/control).
[a]The gene symbols are part of the KEGG pathway "biosynthesis of unsaturated fatty acids."

pathway. We exclusively found differential elongase ratios and no desaturase ratios between control and niacin treatment (data not shown). Furthermore, the differential ratios that were decreased were the C18 to C20 elongation ratios, while the C20 to C22 ratios were increased, indicating a possible increase in the metabolism and processing of essential FAs toward downstream PUFAs in gWAT from niacin-treated mice (**Table 3**). Given that niacin did not elevate the fractional content of the downstream PUFAs of the essential FAs, we studied whether niacin treatment increased PUFA secretion from freshly isolated adipocytes.

Although the fraction of medium-chain fatty acids (MCFAs; C10:0/C12:0/C14:0) was also increased in gWAT after niacin, adipocyte release of these MCFAs was not different (supplementary Fig. VII). Of the PUFAs, both ALA and LA were secreted in equal amounts for control and niacin-treated adipocytes (**Fig. 2A**). Interestingly, downstream metabolic products of the essential n-3 FA ALA, namely EPA (nonsignificant after FDR correction) and DHA, were secreted to a greater extent after niacin treatment.

Liver PUFA biosynthesis gene expression and FA composition

As adipose tissue and the liver are the main sites of NEFA processing, we also examined the effects of prolonged niacin on the liver. We found by using qPCR that *Elovl5* and *Fads2* expression were unaffected by niacin treatment, while *Elovl6* expression was downregulated (Fig. 1). Liver FA composition did not differ between control and niacin-treated mice (supplementary Fig. II and Table III), and neither did the substrate/product ratios relevant for PUFA biosynthesis (data not shown). Although the PUFA fractions of the livers from niacin-treated mice went in the inverse direction as seen in gWAT, this effect was nonsignificant.

Plasma PUFAs and oxylipins

In addition to measuring PUFA levels in adipocyte medium ex vivo, we also examined PUFA levels in plasma by LC-MS/MS. Niacin reduced circulating levels of ALA and tended to increase the levels of its downstream product DHA [Fig. 2B and supplementary Table IV; DHA was not

TABLE 2. Pathways regulated on gene expression level by niacin in the gWAT according to global test

KEGG ID	KEGG Pathway Name	*P*	FDR *q* Value
map01040	Biosynthesis of unsaturated fatty acids	1.81E−05	0.00381
map00310	Lysine degradation	7.97E−04	0.16654
map00900	Terpenoid backbone biosynthesis	1.02E−03	0.21273
map00620	Pyruvate metabolism	1.09E−03	0.22603
map00100	Steroid biosynthesis	1.32E−03	0.27205

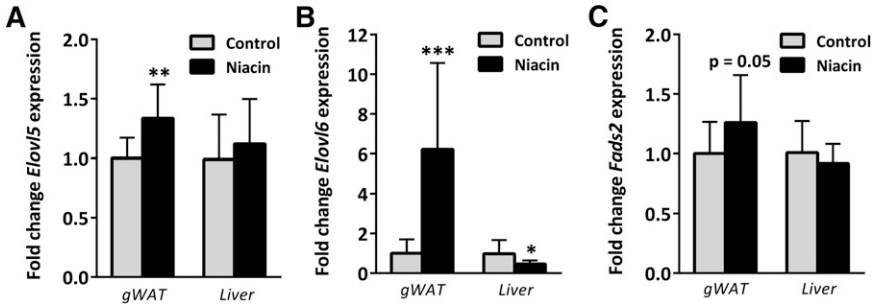

Fig. 1. Gene expression by qPCR of gWAT and liver tissue isolated from unfasted control and niacin-treated mice. *Elovl5* (A), *Elovl6* (B), and *Fads2* (C) mRNA levels expressed as fold change from control. * $P < 0.05$, ** $P < 0.01$, *** $P < 0.001$ compared with control.

significant (NS) after FDR correction]. EPA levels were not affected by niacin. We next examined the ratio of DHA over AA as a surrogate marker for PUFA-associated cardiovascular risk (27–29) and found that the ratio was shifted toward DHA, both in adipocyte medium and in plasma (**Fig. 3A**). PUFA-derived oxylipin signaling molecules were also measured in the plasma (Fig. 3B and supplementary Table IV). The AA metabolite prostaglandin D_2 was not affected by niacin treatment, whereas thromboxane B_2 levels increased (NS after FDR correction). The AA metabolite leukotriene E_4 decreased after niacin treatment (NS after FDR correction), whereas 12-HETE levels remained unchanged. The n-3 PUFA-derived diol metabolite 19,20-diHDPA produced by cytochrome P450 (CYP) was significantly increased. Due to the increase in DHA levels, we investigated the presence of DHA-derived resolvins (30), which could, however, not be detected by our approach.

DISCUSSION

The current study demonstrates for the first time that prolonged niacin treatment results in an upregulation of the n-3 PUFA synthesis pathway in adipose tissue. Gene expression analysis of gWAT showed that our hyperlipidemic mouse model responded to niacin by upregulating genes involved in the unsaturated FA biosynthesis. FA composition analysis corroborated the increased PUFA synthesis. A higher degree of n-3 PUFA secretion from prolonged niacin-treated adipocytes was seen, which was also reflected in increased n-3 PUFA plasma levels. Markedly, the plasma levels of n-3 PUFA-derived oxylipins produced by CYP and hydrolyzed by soluble epoxy hydrolases were increased. Oxylipins produced by CYP from n-3 PUFAs and the n-3 PUFAs themselves suggest a beneficial vascular health profile, which might contribute to the prolonged niacin-induced atheroprotective effect.

Gene expression analysis of the gWATof hyperlipidemic mice treated with niacin for 15 weeks demonstrated an upregulation of the "biosynthesis of unsaturated fatty acids" pathway, mostly by upregulation of *Elovl6*, *Tecr*, and *Elovl5*. All three genes are involved in FA elongation, not desaturation (as shown in **Fig. 4** and Table 3). This discovery was confirmed by qPCR, but also by gWAT FA composition and FA ratio analysis, which all pointed toward PUFA elongation. This increase in PUFA elongation was seen in adipose tissue, but not in liver tissue, where a more inverse trend toward PUFA accumulation could be seen in the FA composition. When examining the PUFA secretion of adipocytes isolated from these mice, we found that specifically end products of n-3 PUFA biosynthesis were secreted to a higher degree, as seen by DHA (C22:6) and also by EPA (C20:5)

TABLE 3. Gene expression level of significant genes in the "biosynthesis of unsaturated fatty acids" pathway and the associated enzymatic substrate/product ratio of FAs

Gene Name	Symbol	Adjusted *P*	Fold Change	Substrate/Product Ratio	*P*	Fold Change
Trans-2,3-enoyl-CoA reductase	Tecr	0.029	0.498(↑)	General FA elongation		
Elongation of long chain fatty acids 6	Elovl6	0.004	1.371(↑)	C16:0/C18:0	0.416	−0.152(↓)
				C16:1n-9/C18:1n-9	0.019	−0.370(↓)
Elongation of long chain fatty acids 5	Elovl5	0.033	0.405(↑)	C18:3n-3/C20:3n-3	0.007	−0.619(↓)
				C18:4n-3/C20:4n-3	Substrate and product not measured	
				C18:2n-6/C20:2n-6	0.028	−0.540(↓)
				C18:3n-6/C20:3n-6	0.049	−0.390(↓)
Elongation of long chain fatty acids 5 / 2	Elovl5/			C20:5n-3/C22:5n-3	0.155	0.529(↑)
	Elovl2			C20:4n-6/C22:4n-6	0.032	0.387(↑)

The fold changes were calculated as $\log_2$(niacin / control).

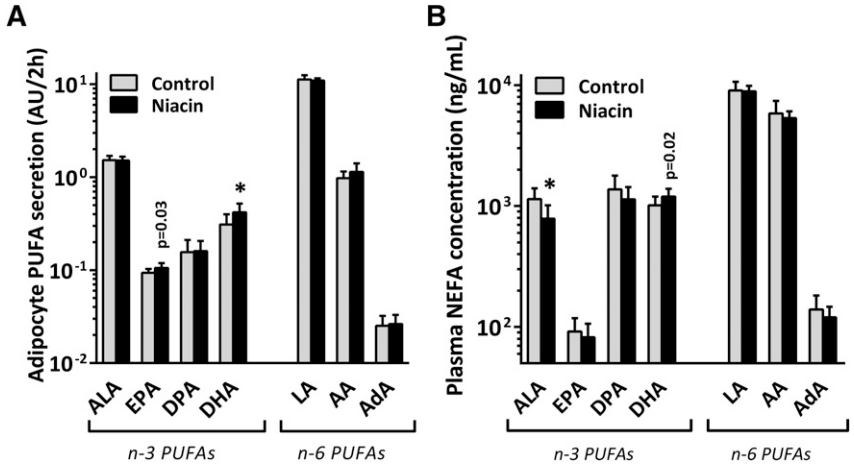

Fig. 2. A: PUFA release from ex vivo isolated adipocytes from control and niacin-treated mice incubated for 2 h in DMEM/F12 medium. B: PUFA concentration in unfasted plasma of control and niacin-treated mice. Mean ± SD; n = 14 for control, n = 13 for niacin. * $P < 0.05$ compared with control gWAT after FDR correction. *P* values listed were before FDR correction. AdA, adrenic acid; DPA, docosapentaenoic acid.

secretion. As the genes involved in PUFA biosynthesis are the same for n-3 PUFAs as for n-6 PUFAs, the specificity for increased n-3 PUFA secretion was puzzling. It is conceivable that the PUFA biosynthesis enzymes have a higher affinity for n-3 PUFAs, as was already shown for zebrafish desaturase enzymes (31). The rat elongase 5 enzyme possesses a higher affinity for n-3 substrates than for n-6 substrates (32), and the mouse equivalent was found to be upregulated in our study. Selective DHA biosynthesis, unlike AA or EPA, requires partial peroxisomal β oxidation (Fig. 4). Although the microarray did not point toward this pathway, increased peroxisomal β oxidation after niacin could lead to preferential DHA synthesis. Aside from preferential n-3 PUFA biosynthesis, preferential mobilization from adipose tissue would also explain an increased n-3 PUFA release. A well-documented phenomenon is selective PUFA release from adipocytes (33), exemplified by fasting-induced preferential n-3 PUFA depletion of adipose tissue TGs (34). Our preliminary results also indicate preferential n-3 PUFA release from adipocytes when (fasting-induced) lipolysis is stimulated by 8Br-cAMP (supplementary Fig. VIIIc). Other potential mechanisms for preferential n-3 PUFA release might be phospholipid hydrolysis, as it has been previously shown that cytosolic phopholipase A_2 releases AA and EPA from phospholipids, whereas the release of DHA from phospholipids requires calcium-independent phopholipase A_2 (35). Although 99% of the FAs are located in the TG fraction, the contribution of the 1% FAs contained in the phospholipid fraction to n-3 PUFA release cannot be excluded. Additional research is required to investigate the underlying mechanisms for the preferential n-3 PUFA release after prolonged niacin treatment.

Adipocyte lipolysis contributes to the free FA pool in the circulation. In the plasma of the niacin-treated animals, we found a tendency for increased levels of the n-3 PUFA DHA in the NEFA pool. Although we do not have direct proof, our data suggest that DHA secretion by adipocytes is the main source of DHA in the plasma. Interestingly, we did not find upregulation of gene expression levels of *Elovl5*, *Elovl6*, or *Fads2*, or any change in FA composition in the livers of the niacin-treated mice, indicating that the niacin-induced PUFA synthesis is selective for adipose tissue.

The n-3 PUFAs have been reported to confer CVD protective abilities via their conversion to anti-inflammatory oxylipins. For example, DHA can be converted to the oxylipin 19(20)-epoxy docosapentaenoic acid [19(20)-EpDPA] by CYP as can be seen in Fig. 4. Likewise, the n-3 PUFA EPA can be converted to 14(15)-epoxy eicosatetraenoic acid [14(15)-EpETE] by CYP. These epoxide metabolites have powerful biological effects on cardiovascular health. This was shown by previous studies where the epoxide metabolism pathway was genetically manipulated (36) or its compounds were

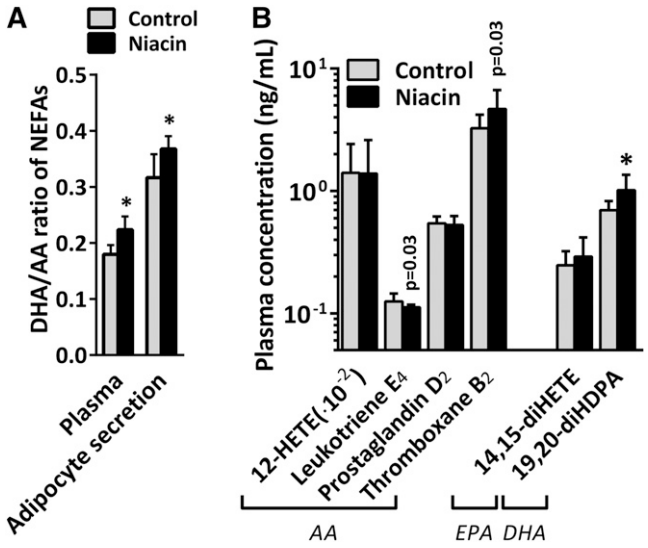

Fig. 3. A: DHA over AA ratio in adipocyte-secreted medium and in plasma. B: Oxylipin concentration in plasma of control and niacin-treated mice. Mean ± SD; n = 14 per group. * $P < 0.05$ compared with control gWAT after FDR correction. *P* values listed were before FDR correction.

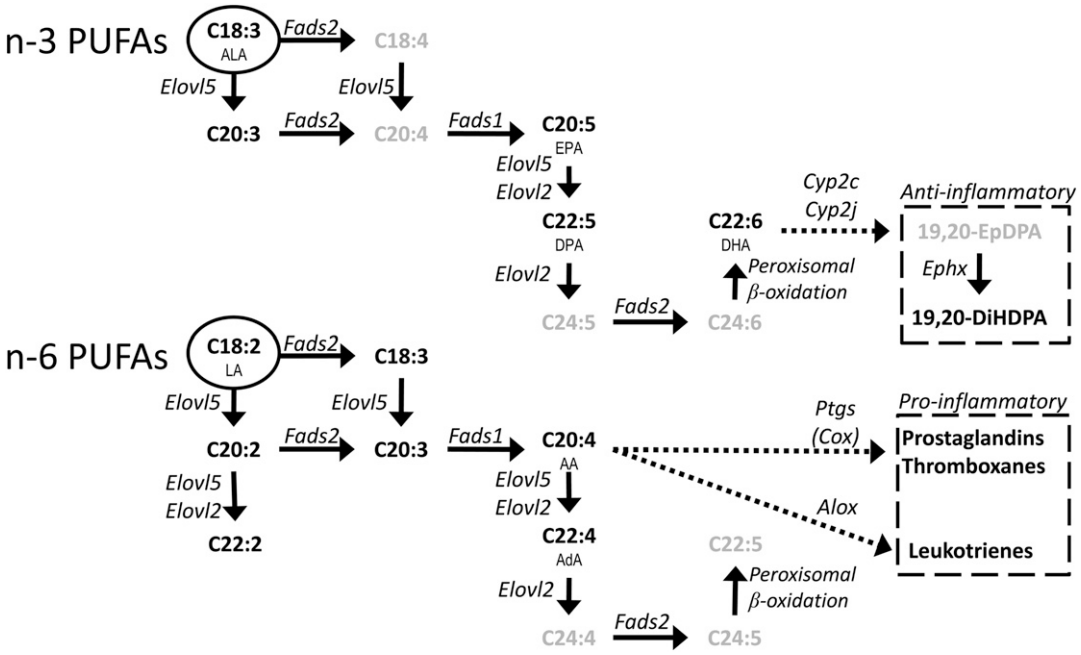

Fig. 4. Schematic overview of the synthesis of PUFAs and the subsequent conversion to a selection of oxylipins. Genes are in italic, metabolites are in bold, and essential FAs are encircled. Metabolites in gray were not measured. Based on the review by Guillou et al. (43).

pharmacologically elevated (37). These studies showed the importance of epoxy metabolites in resolving inflammation, preserving vascular tone, and general vascular homeostasis. The biologically active 19(20)-EpDPA and 14(15)-EpETE can be hydrolyzed by soluble epoxy hydrolases (encoded by the *Ephx2* gene in mice) to their respective diol metabolites 19,20-diHDPA and 14,15-diHETE. The levels of both these diol products were increased in plasma of niacin-treated animals. The hydrolyzed diol metabolites have a far lower biological effect than their epoxide metabolites but are more stable and can be detected in plasma by LC-MS/MS. Although we did not directly measure whether the levels of the bioactive epoxy metabolites 19(20)-EpDPA or 14(15)-EpETE were increased after niacin treatment, we found a positive correlation in plasma between the precursor and diol metabolite of 19(20)-EpDPA (DHA and 19,20-diHDPA) in niacin-treated mice (supplementary Fig. III). This correlation suggests that the levels of 19(20)-EpDPA must also have increased after niacin treatment.

In general, the anti-inflammatory oxylipins such as epoxy metabolites produced by CYP (high affinity for n-3 PUFAs) are balanced by the proinflammatory oxylipins such as those produced by COXs and arachidonate lipoxygenases (both with high affinity for n-6 PUFAs, such as AA) (38). Prolonged niacin treatment did not dramatically affect AA-derived oxylipin levels, although there was a tendency toward decreased levels of leukotriene E_4, a lipoxygenase pathway product stimulating inflammation, and toward increased levels of thromboxane B_2, a COX product stimulating coagulation.

Acute treatment of mouse adipocytes with niacin did not lead to an increased release of DHA or AA, nor a change in the ratio of DHA/AA in the adipocyte-conditioned medium (supplementary Fig. IX). Acute niacin treatment, however, is a well-known trigger for AA-derived oxylipin synthesis in the skin. Irritative subcutaneous skin flushing is a common acute side effect of niacin, induced by COX product prostaglandin D_2 (39) in Langerhans cells and keratinocytes. As mentioned previously, we did not see an increase in proinflammatory prostaglandins after prolonged niacin treatment. These results are in line with results by Stern et al. (17) and suggest tolerance for flushing after prolonged niacin treatment. It is possible that the tolerance for flushing after prolonged niacin is mediated via n-3 PUFAs as suggested by VanHorn et al. (40). Whether there is a role for anti-inflammatory n-3 PUFA-derived oxylipins after acute niacin remains unclear. Inceoglu et al. (41) have acutely administered niacin to mice being treated with a soluble epoxide hydrolase inhibitor, which resulted in a blunted flushing response compared with wild-type mice, while acute prostaglandin D_2 treatment did not blunt flushing. These results support a role for CYP epoxide metabolites not only after prolonged niacin treatment, but also acutely in inhibiting the flushing response by niacin. Flushing severity also suggests an important balance between pro- and anti-inflammatory oxylipins, which can be modulated by niacin treatment. Most likely, the n-6-derived oxylipins prevail during acute niacin treatment, while after prolonged niacin treatment the n-3-derived oxylipins prevail.

Plasma DHA/AA ratio has been shown to be a diagnostic marker for PUFA-associated cardiovascular health (27–29). In addition to being metabolized to anti-inflammatory oxylipins, n-3 PUFAs confer their CVD protective abilities by direct competition with n-6 PUFAs. VanHorn et al. (40) have described that DHA supplementation increases the DHA/AA ratio in membrane phospholipids of Langerhans cells, thereby diminishing the relative availability of AA for proinflammatory prostaglandin synthesis. As a low n-3/n-6

ratio is associated with a risk for CVD, increasing the ratio by supplementary n-3 PUFAs has been posed as a treatment target (42). In our study, we see that the DHA/AA ratio has increased toward the anti-inflammatory DHA side without supplementary n-3 PUFAs. We have seen this increased DHA/AA ratio in both the ex vivo adipocyte PUFA secretion profile and in the in vivo plasma NEFA profile of niacin-treated mice. These effects of niacin on adipose tissue and plasma PUFAs and oxylipins pose a potential contributing mechanism by which niacin treatment reduces cholesterol levels and CVD risk. Although we used mice in this study that are human-like with respect to lipoprotein profile, it remains to be investigated whether there are changes in the plasma DHA/AA ratio in humans treated with niacin.

In conclusion, prolonged niacin treatment of our hyperlipidemic mouse model with niacin resulted in upregulation of the entire biosynthesis of unsaturated fatty acids pathway in gWAT, increased n-3 PUFA secretion from the adipocytes, and an increased plasma level of n-3 PUFAs and their anti-inflammatory oxylipins, which together point toward an atheroprotective plasma profile induced by prolonged niacin treatment.

The authors thank Dr. Makoto Arita from the Department of Health Chemistry Graduate School of Pharmaceutical Sciences, University of Tokyo, Japan, for the kind gift of RvE1, RvE2, 18S-RvE3, and 18R-RvE3 used as standard material in the LC-MS/MS platform used.

REFERENCES

1. Bruckert, E., J. Labreuche, and P. Amarenco. 2010. Meta-analysis of the effect of nicotinic acid alone or in combination on cardiovascular events and atherosclerosis. *Atherosclerosis.* **210:** 353–361.
2. Morgan, J. M., D. M. Capuzzi, R. I. Baksh, C. Intenzo, C. M. Carey, D. Reese, and K. Walker. 2003. Effects of extended-release niacin on lipoprotein subclass distribution. *Am. J. Cardiol.* **91:** 1432–1436.
3. Hernandez, M., S. D. Wright, and T-Q. Cai. 2007. Critical role of cholesterol ester transfer protein in nicotinic acid-mediated HDL elevation in mice. *Biochem. Biophys. Res. Commun.* **355:** 1075–1080.
4. Wanders, D., E. C. Graff, B. D. White, and R. L. Judd. 2013. Niacin increases adiponectin and decreases adipose tissue inflammation in high fat diet-fed mice. *PLoS ONE.* **8:** e71285.
5. Wu, B. J., K. Chen, P. J. Barter, and K. A. Rye. 2012. Niacin inhibits vascular inflammation via the induction of heme oxygenase-1. *Circulation.* **125:** 150–158.
6. Chen, X., N. Iqbal, and G. Boden. 1999. The effects of free fatty acids on gluconeogenesis and glycogenolysis in normal subjects. *J. Clin. Invest.* **103:** 365–372.
7. Kasalický, J., M. Konopková, and F. Melichar. 2001. 18F-fluorodeoxyglucose accumulation in the heart, brain and skeletal muscle of rats; the influence of time after injection, depressed lipid metabolism and glucose-insulin. *Nucl. Med. Rev. Cent. East. Eur.* **4:** 39–42.
8. Kaushik, S. V., E. P. Plaisance, T. Kim, E. Y. Huang, A. J. Mahurin, P. W. Grandjean, and S. T. Mathews. 2009. Extended-release niacin decreases serum fetuin-A concentrations in individuals with metabolic syndrome. *Diabetes Metab. Res. Rev.* **25:** 427–434.
9. O'Neill, M., M. J. Watt, G. J. F. Heigenhauser, and L. L. Spriet. 2004. Effects of reduced free fatty acid availability on hormone-sensitive lipase activity in human skeletal muscle during aerobic exercise. *J. Appl. Physiol.* **97:** 1938–1945.
10. Oh, Y. T., K-S. Oh, Y. M. Choi, A. Jokiaho, C. M. Donovan, S. Choi, I. Kang, and J. H. Youn. 2011. Continuous 24-h nicotinic acid infusion in rats causes FFA rebound and insulin resistance by altering gene expression and basal lipolysis in adipose tissue. *Am. J. Physiol. Endocrinol. Metab.* **300:** E1012–E1021.
11. Quabbe, H-J., A. S. Luyckx, M. L'age, and C. Schwarz. 1983. Growth hormone, cortisol, and glucagon concentrations during plasma free fatty acid depression: different effects of nicotinic acid and an adenosine derivative (BM 11.189). *J. Clin. Endocrinol. Metab.* **57:** 410–414.
12. Watt, M. J., A. G. Holmes, G. R. Steinberg, J. L. Mesa, B. E. Kemp, and M. A. Febbraio. 2004. Reduced plasma FFA availability increases net triacylglycerol degradation, but not GPAT or HSL activity, in human skeletal muscle. *Am. J. Physiol. Endocrinol. Metab.* **287:** E120–E127.
13. Hanson, J., A. Gille, S. Zwykiel, M. Lukasova, B. Ý. E. Clausen, K. Ahmed, S. Tunaru, A. Wirth, and S. Offermanns. 2010. Nicotinic acid- and monomethyl fumarate-induced flushing involves GPR109A expressed by keratinocytes and COX-2-dependent prostanoid formation in mice. *J. Clin. Invest.* **120:** 2910–2919.
14. Gadegbeku, C. A., A. Dhandayuthapani, M. Z. Shrayyef, and B. M. Egan. 2003. Hemodynamic effects of nicotinic acid infusion in normotensive and hypertensive subjects. *Am. J. Hypertens.* **16:** 67–71.
15. Wang, W., A. Basinger, R. A. Neese, M. Christiansen, and M. K. Hellerstein. 2000. Effects of nicotinic acid on fatty acid kinetics, fuel selection, and pathways of glucose production in women. *Am. J. Physiol. Endocrinol. Metab.* **279:** E50–E59.
16. Heemskerk, M. M., S. A. van den Berg, A. C. Pronk, J. B. van Klinken, M. R. Boon, L. M. Havekes, P. C. Rensen, K. W. van Dijk, and V. van Harmelen. 2014. Long-term niacin treatment induces insulin resistance and adrenergic responsiveness in adipocytes by adaptive downregulation of phosphodiesterase 3B. *Am. J. Physiol. Endocrinol. Metab.* **306:** E808–E813.
17. Stern, R. H., J. D. Spence, D. J. Freeman, and A. Parbtani. 1991. Tolerance to nicotinic acid flushing. *Clin. Pharmacol. Ther.* **50:** 66–70.
18. Choi, S., H. Yoon, K-S. Oh, Y. T. Oh, Y. I. Kim, I. Kang, and J. H. Youn. 2011. Widespread effects of nicotinic acid on gene expression in insulin-sensitive tissues: implications for unwanted effects of nicotinic acid treatment. *Metabolism.* **60:** 134–144.
19. Westerterp, M., C. C. van der Hoogt, W. de Haan, E. H. Offerman, G. M. Dallinga-Thie, J. W. Jukema, L. M. Havekes, and P. C. Rensen. 2006. Cholesteryl ester transfer protein decreases high-density lipoprotein and severely aggravates atherosclerosis in APOE*3-Leiden mice. *Arterioscler. Thromb. Vasc. Biol.* **26:** 2552–2559.
20. Kühnast, S., M. C. Louwe, M. M. Heemskerk, E. J. Pieterman, J. B. van Klinken, S. A. van den Berg, J. W. Smit, L. M. Havekes, P. C. Rensen, J. W. van der Hoorn, et al. 2013. Niacin reduces atherosclerosis development in APOE*3Leiden.CETP mice mainly by reducing nonHDL-cholesterol. *PLoS ONE.* **8:** e66467.
21. Du, P., W. A. Kibbe, and S. M. Lin. 2008. lumi: a pipeline for processing Illumina microarray. *Bioinformatics.* **24:** 1547–1548.
22. Smyth, G. K. 2004. Linear models and empirical Bayes methods for assessing differential expression in microarray experiments. *Stat. Appl. Genet. Mol. Biol.* **3:** 3.
23. Goeman, J. J., S. A. van de Geer, F. de Kort, and H. C. van Houwelingen. 2004. A global test for groups of genes: testing association with a clinical outcome. *Bioinformatics.* **20:** 93–99.
24. Kloos, D. P., E. Gay, H. Lingeman, F. Bracher, C. Müller, O. A. Mayboroda, A. M. Deelder, W. M. A. Niessen, and M. Giera. 2014. Comprehensive GC–MS analysis of fatty acids and sterols using sequential one-pot silylation: quantification and isotopologue analysis. *Rapid Commun. Mass Spectrom.* **28:** 1507–1514.
25. Giera, M., A. Ioan-Facsinay, R. Toes, F. Gao, J. Dalli, A. M. Deelder, C. N. Serhan, and O. A. Mayboroda. 2012. Lipid and lipid mediator profiling of human synovial fluid in rheumatoid arthritis patients by means of LC-MS/MS. *Biochim. Biophys. Acta.* **1821:** 1415–1424.
26. Yang, R., N. Chiang, S. F. Oh, and C. N. Serhan. 2011. Metabolomics-lipidomics of eicosanoids and docosanoids generated by phagocytes. *Curr. Protoc. Immunol.* **95:** 14.26.1–14.26.26.
27. Nozue, T., S. Yamamoto, S. Tohyama, K. Fukui, S. Umezawa, Y. Onishi, T. Kunishima, A. Sato, T. Nozato, S. Miyake, et al. 2014. Low serum docosahexaenoic acid is associated with progression of coronary atherosclerosis in statin-treated patients with diabetes mellitus: results of the treatment with statin on atheroma regression evaluated by intravascular ultrasound with virtual histology (TRUTH) study. *Cardiovasc. Diabetol.* **13:** 13.

28. Nishizaki, Y., K. Shimada, S. Tani, T. Ogawa, J. Ando, M. Takahashi, M. Yamamoto, T. Shinozaki, K. Miyauchi, K. Nagao, et al. 2014. Significance of imbalance in the ratio of serum n-3 to n-6 polyunsaturated fatty acids in patients with acute coronary syndrome. *Am. J. Cardiol.* **113:** 441–445.
29. Dohi, T., K. Miyauchi, S. Okazaki, T. Yokoyama, H. Tamura, T. Kojima, K. Yokoyama, T. Kurata, and H. Daida. 2011. Long-term impact of mild chronic kidney disease in patients with acute coronary syndrome undergoing percutaneous coronary interventions. *Nephrol. Dial. Transplant.* **26:** 2906–2911.
30. Serhan, C. N., and N. A. Petasis. 2011. Resolvins and protectins in inflammation resolution. *Chem. Rev.* **111:** 5922–5943.
31. Hastings, N., M. Agaba, D. R. Tocher, M. J. Leaver, J. R. Dick, J. R. Sargent, and A. J. Teale. 2001. A vertebrate fatty acid desaturase with Δ5 and Δ6 activities. *Proc. Natl. Acad. Sci. USA.* **98:** 14304–14309.
32. Gregory, M. K., R. A. Gibson, R. J. Cook-Johnson, L. G. Cleland, and M. J. James. 2011. Elongase reactions as control points in long-chain polyunsaturated fatty acid synthesis. *PLoS ONE.* **6:** e29662.
33. Raclot, T. 2003. Selective mobilization of fatty acids from adipose tissue triacylglycerols. *Prog. Lipid Res.* **42:** 257–288.
34. Nieminen, P., A-M. Mustonen, V. Kärjä, J. Asikainen, and K. Rouvinen-Watt. 2009. Fatty acid composition and development of hepatic lipidosis during food deprivation—mustelids as a potential animal model for liver steatosis. *Exp. Biol. Med. (Maywood).* **234:** 278–286.
35. Strokin, M., M. Sergeeva, and G. Reiser. 2003. Docosahexaenoic acid and arachidonic acid release in rat brain astrocytes is mediated by two separate isoforms of phospholipase A2 and is differently regulated by cyclic AMP and Ca2+. *Br. J. Pharmacol.* **139:** 1014–1022.
36. Imig, J. D. 2012. Epoxides and soluble epoxide hydrolase in cardiovascular physiology. *Physiol. Rev.* **92:** 101–130.
37. Askari, A. A., S. Thomson, M. L. Edin, F. B. Lih, D. C. Zeldin, and D. Bishop-Bailey. 2014. Basal and inducible anti-inflammatory epoxygenase activity in endothelial cells. *Biochem. Biophys. Res. Commun.* **446:** 633–637.
38. Fischer, R., A. Konkel, H. Mehling, K. Blossey, A. Gapelyuk, N. Wessel, C. von Schacky, R. Dechend, D. N. Muller, M. Rothe, et al. 2014. Dietary omega-3 fatty acids modulate the eicosanoid profile in man primarily via the CYP-epoxygenase pathway. *J. Lipid Res.* **55:** 1150–1164.
39. Serebruany, V., A. Malinin, D. Aradi, W. Kuliczkowski, N. B. Norgard, and W. E. Boden. 2010. The in vitro effects of niacin on platelet biomarkers in human volunteers. *Thromb. Haemost.* **104:** 311–317.
40. VanHorn, J., J. D. Altenburg, K. A. Harvey, Z. Xu, R. J. Kovacs, and R. A. Siddiqui. 2012. Attenuation of niacin-induced prostaglandin D(2) generation by omega-3 fatty acids in THP-1 macrophages and Langerhans dendritic cells. *J. Inflamm. Res.* **5:** 37–50.
41. Inceoglu, A. B., H. L. Clifton, J. Yang, C. Hegedus, B. D. Hammock, and S. Schaefer. 2012. Inhibition of soluble epoxide hydrolase limits niacin-induced vasodilation in mice. *J. Cardiovasc. Pharmacol.* **60:** 70–75.
42. Simopoulos, A. P. 2008. The importance of the omega-6/omega-3 fatty acid ratio in cardiovascular disease and other chronic diseases. *Exp. Biol. Med. (Maywood).* **233:** 674–688.
43. Guillou, H., D. Zadravec, P. G. P. Martin, and A. Jacobsson. 2010. The key roles of elongases and desaturases in mammalian fatty acid metabolism: insights from transgenic mice. *Prog. Lipid Res.* **49:** 186–199.